

# Process Characterization of One Hundred Micron Thick Photoresist Films

**Warren W. Flack, Sylvia White, Bradley Todd**  
**Ultratech Stepper, Inc.**  
**San Jose, CA 95134**

The number of lithographic applications that require the use of photoresists thickness of one hundred microns or more is rapidly increasing. Extremely large structure heights and high aspect ratios are often required for micro-electrodeposition of mechanical components such as coils, cantilevers and valves. These ultra-thick photoresists can also be used as a mold in micro-electromechanical systems (MEMS). Ultra-thick photoresists are also used in bump bond applications to define the size and location of the bonds for advanced flipchip packaging.

Optical steppers offer significant advantages for processing these ultra-thick photoresists due to the tighter overlay and improved critical dimension (CD) control possible compared with full wafer optical tools. A stepper has an additional advantage with ultra-thick photoresist structures since the focus can be adjusted at various levels into a thick film, which will result in improved wall angles and enhanced aspect ratios.

The process optimization required to obtain high aspect ratio structures in these ultra-thick photoresist films is extremely challenging. The aspect ratios far exceed those encountered in advanced submicron lithography for integrated circuit (IC) manufacturing. Physical properties such as adhesion and structural rigidity play a critical role in obtaining high aspect ratios in dense line and space patterns. The photoresist optical properties and developer characteristics are more significant for patterning isolated structures. Unlike typical photoresists for IC manufacturing, lithography modeling and characterization tools are not available for photoresist films in this thickness range.

For this study the performance of three commercially available positive and negative ultra-thick photoresists are examined at a thickness of one hundred microns using both high throughput i-line and gh-line lithography systems optimized for thick photoresist processing. The photoresists used in this study are selected to represent the full range of chemistries available from different manufacturers. Basic photoresist characterization techniques established for thin films in IC manufacturing are applied to these ultra-thick photoresist films. Cross sectional SEM analysis, process linearity, Bossung plots and process window plots are used to establish relative lithographic capabilities of each photoresist. The trade-offs between the various photoresist chemistries are reviewed and compared with the process requirements for high aspect ratio applications.

**Key Words:** ultra-thick photoresist, MEMS, photoresist characterization, resolution

## 1.0 INTRODUCTION

The MEMS market is growing rapidly by expanding into various areas such as medical devices including single use health monitors, automotive applications such as airbag accelerometers and actuators for automobile braking and suspension systems [1,2,3]. The historical machining methods used to create larger mechanical devices are

not amenable to use at the micron size geometries that characterize MEMS devices. EDM (electronic discharge machining), diamond milling, abrasive jets and laser machining have been used for many years to create the smallest mechanical devices and represent an extension of the standard machining processes [4,5]. These methods have not been particularly adaptable to volume manufacturing of low cost items. An exception to this is the use of laser machining for inkjet nozzle production. Inkjet nozzles are extremely simple structures and general application of lasers to volume production has not been widely accepted for more complex structures.

LIGA (Lithografie Galvanik Abformung) processing, thin film head (TFH) fabrication for hard disk drives and flipchip packaging make use of thick photoresists to form molds for electroplating of metals [6]. Electroplating metals for micro-scale features itself does not present new technical challenges, however, the fabrication of the consumable molds requires high precision tolerances. LIGA processing of high aspect ratio features in thick polymer films has been under development for many years [7,8]. Some MEMS products have had commercial success with LIGA processing and are currently used to make low volume parts. LIGA is capable of making well controlled high aspect ratio polymer molds, but has the economic disadvantage of requiring the use of X-ray synchrotron sources that are not readily available. Another approach to solving the problem of high aspect ratio molds finds its roots in the use of thick photoresists and optical lithography equipment originally developed for production of semiconductor devices. Steppers, full wafer scanners, and contact printers are widely used in the microelectronic industry and are highly evolved production tools. A stepper offers tighter overlay and improved CD in comparison to a contact printer or full wafer scanner. Stepper systems can also adjust the focal height relative to the surface of the thick photoresist, resulting in improved wall angles and better aspect ratios as compared to contact lithography tools. Ultra-thick photoresists typically require a large exposure dosage for high aspect ratio lithography. For this reason, it is advantageous to utilize a stepper with a broad band exposure system to maximize the illumination intensity at the wafer plane. Broad-band steppers have been used for some years in manufacturing TFH devices for use in computer hard disk drives where ten microns of photoresist with features less than two microns are common [9]. More recently, effort has been focused on extending this highly evolved production method to thicker photoresists with greater aspect ratios to make advanced flipchip packaging [10,11].

Manufacturing tolerances for MEMS structures can be quite different from those associated with microelectronics. The industry standard for geometrical tolerances for the microelectronics industry is only specified in one dimension, linewidth. Contrast this with the case of a parallel plate capacitive drive or sensor where the dimensions of the airgap between the plates are the critical parameters. This represents either a two or three dimensional control situation typically specified by wall angle and profile as well as linewidth [12,13,14,15].

Controlling aspect ratio and linewidth for structures with aspect ratios larger than 3:1 is a challenging use of photolithography equipment and photoresists. The aerial image for most steppers has been optimized for making submicron linewidths in one micron thick photoresists by maximizing the lens numerical aperture (NA) for a small optical field size [16]. Steppers for MEMS fabrication need to be optimized for larger geometries while retaining both depth of focus (DOF) and larger exposure fields. Photoresist performance, like stepper performance, has generally been optimized over recent years for achieving the smallest geometries possible. Some newer photoresist formulations are available that have properties more tailored for making high aspect ratio structures required for electroplating molds [17,18]. Three commercially available photoresists representing a range of available chemistries were chosen for examination in this study. The photoresists chosen were novalac based AZ PLP-100, polyhydroxy styrene based NR9-8000 and epoxy based SU8-10. The NR9-8000 and SU8-10 are negative acting photoresists. Frequently these photoresists are broadband or deep UV sensitive materials. Because of this, both i-line and g-line steppers were used for photoresist characterization.

## 2.0 EXPERIMENTAL METHODS

### 2.1 Reticle Design and Manufacture

The Ultratech 1X reticle used for this study is designed primarily to support easy cross sectional SEM metrology for MEMS applications. The reticle consists of two fields of 42.8 by 21.4 mm, one of each polarity to support both positive and negative acting photoresists. Each field contains horizontal and vertical grouped line and space patterns from 2 to 20  $\mu\text{m}$  in 2  $\mu\text{m}$  size increments, and from 25 to 40  $\mu\text{m}$  in 5  $\mu\text{m}$  size increments. Figure 1 shows a sample cell containing vertical lines. Both equal line and space patterns and isolated lines are included for all structure sizes. Each isolated line is separated from its nearest neighbors by a minimum of five times the linewidth. All of the line structures are 5 mm in length to facilitate cross sectional SEM analysis. In order to increase the mechanical integrity of these long lines, they are placed in a zigzag pattern with a ten degree angle and a seven to one length to width ratio for each line segment. The reticle was written on an advanced e-beam system using a high resolution PBS resist. There is no data biasing applied to the design data and CDs are held to within  $\pm 0.03 \mu\text{m}$  of a nominal 2.0  $\mu\text{m}$  chrome line. Reticle CD information was also obtained for all line sizes on both fields to establish the process linearity in reticle fabrication.

### 2.2 Lithography Equipment

Lithography for each photoresist evaluated in this study was performed on either an Ultratech Stepper Saturn III Wafer Stepper<sup>®</sup> or Ultratech Stepper Titan II Wafer Stepper<sup>®</sup> depending upon its optimal spectral sensitivity. The Saturn III stepper and the Titan II stepper are based on the 1X Wynne-Dyson lens design employing Hg broadband illumination [19]. The Saturn i-line spectrum is from 355 to 375 nm and the Titan gh-line spectrum is from 390 to 450 nm. The optical specifications of both lithography systems used in this study are shown in Table 1. Both steppers use Machine Vision System (MVS), a pattern recognition system, which can align to a wide variety of structures on the wafer. Exposure uniformity was verified prior to collecting the experimental data and was found to be 1.2 percent across the entire field. Multiple wafers were exposed in a focus/exposure pattern consisting of a seven by seven field array as illustrated in Figure 2. Nominal exposure dose was determined by measuring isolated spacewidth patterns with a Hitachi S-7280H metrology SEM. A 50 percent signal threshold criteria was selected for the determination of the linewidth CD for both the negative and positive photoresists.

### 2.3 Processing Conditions

SEMI standard ultra-flat silicon wafers were used for this study. The 150 mm wafers were pre-treated according to recommendations by the photoresist manufacturers as described in Tables 3, 4 and 5 for each photoresist. Three commercially available ultra-thick photoresist products were used for this investigation: Clariant Corporation AZ PLP-100<sup>®</sup> positive photoresist, Futurrex Inc. NR9-8000<sup>®</sup> negative photoresist, and Microlithography Chemical Corporation (MCC) SU8-10<sup>®</sup> negative photoresist. These photoresists were selected because of the diversity of their photo-chemistries as discussed in Section 3.0. Each photoresist was coated to the 100  $\mu\text{m}$  target thickness using the process and equipment described in Tables 3, 4, and 5. Photoresist thickness and uniformity were measured on a Dektak 3030 surface profilometer measurement system. Note that SU8-10 photoresist was coated with a single coating step while the other two photoresist required multiple coatings to achieve the desired photoresist thickness.

All wafers used for this work were new. This was to prevent any adhesion problems from previous adhesion promoters or cleaning processes. Only the AZ PLP-100 required an HMDS vapor prime of the wafers. All post exposure and softbakes of the wafers conducted on Solitec hotplates were accomplished with a maximum exhaust

and covers removed. It was observed that solvent can condense on the underside of a cover and drip back onto the wafers. Without a high level of exhaust the solvent will not evaporate out of the film adequately.

For the SU8-10 the manufacturer specified that the wafers be cooled slowly after both post exposure bake and softbake to prevent any cracking of the film. This was accomplished by resting the wafers into a boat in a horizontal position until they reached ambient temperature. For consistency, wafers coated with all three materials were processed in this manner. However it was observed that the AZ PLP-100 was particularly susceptible to cracking. When the AZ PLP-100 wafers were put onto the microscope for visual examination, the film would frequently crack from contact with the chuck. After evaluation in the SEM, it was noted that most of the cracking appeared to be superficial and did not penetrate much beyond the surface of the film.

## 2.4 Data Analysis

Wafers coated with each of the three photoresists were exposed on either the gh-line or the i-line lithography system based on optimal spectral sensitivity of the individual photoresist. All wafers were visually inspected and measured on a Hitachi S-7280H metrology SEM to determine the photoresist linearity over a range of linesizes. CD measurements of isolated spaces were taken at 1000x magnification. A range of spacewidths were measured top-down on the S-7280H over the entire focus and exposure matrix as illustrated in Figure 2. This CD data was entered into a spreadsheet and analyzed using Prodata<sup>®</sup> software by Finle Technologies. Both Bossung plots and process window plots were generated using 10 percent CD control criteria. Cross sectional SEM micrographs were obtained to illustrate masking linearity for isolated spaces. The CD linearity data is also plotted for each photoresist. The results from the data analysis are discussed in Section 3.0.

## 3.0 RESULTS AND DISCUSSIONS

### 3.1 Linearity Analysis

Figure 3 shows the mask linearity for each of the three photoresists evaluated. This graph shows that the printed feature size is linear with respect to the reticle feature size and is predictable within the range of error shown. This figure was constructed using top down SEM data for isolated spaces and is a best fit plot of the data to the equation:

$$y = x + b \quad (1)$$

where  $y$  is the measured spacewidth,  $x$  is the reticle spacewidth and  $b$  is the mask bias. The mask bias and goodness of fit for each of the photoresists is shown in Table 2. Note that the mask bias is negative for the two negative photoresists (NR9-8000 and SU8-10) and positive for the positive photoresist, AZ PLP-100.

A region of linear correlation between photomask features and printed features allows designers to utilize a range of device geometries on a single photolithography level with a single biasing offset between the mask feature and the printed feature. Mask linearity will be discussed in more detail for each photoresist in subsequent sections.

### 3.2 MCC SU8-10

MCC SU8-10 is a negative acting, epoxy-type, Shell Chemical EPON<sup>®</sup> resin based photoresist. Previous evaluation of SU8-5 on the Titan II stepper showed minimal photo-sensitivity in the gh-line spectrum [17,18]. Therefore, the Saturn III was chosen for continuing evaluation of this photoresist at 100  $\mu\text{m}$  thickness. The film retention analysis published in a previous study showed an average value of 90 percent of the pre-develop thickness measured over the exposure doses used for this study, indicating excellent film retention [18].

Wafers were imaged on the Saturn III stepper with exposure energies ranging from 300 mJ/cm<sup>2</sup> to 600 mJ/cm<sup>2</sup> and focus offsets ranging from -50 μm to +15 μm. SU8-10 demonstrated a 7.0 μm resolution for isolated spacewidths in the i-line as illustrated by the cross sectional SEM micrographs shown in Figure 4a. Sidewall angles were not calculated because at 100 μm photoresist thickness any high aspect ratio cleared features have wall angles very close to 90 degrees and this normal figure of merit does not differentiate between results of the three photoresists. No curvature or foot was observed at the base of the photoresist. A maximum aspect ratio of 14.3:1 (photoresist thickness / minimum space width resolved) was observed.

SU-8 exhibits well behaved process characteristics. Figure 4b shows Bossung plots for 15 and 9.0 μm spacewidth features. The grey box in each plot shows a ten percent CD latitude for the given spacewidth. The Prodata software performed a polynomial regression analysis on exposure and focus to determine the CD curves for each exposure dose. The process window data shown in Figure 4c was generated from Bossung data in Figure 4b for the 15 and 9.0 μm features. The envelope demonstrates a ten percent control limits for the given spacewidth. The shaded rectangle reflects the largest rectangular process window with a 15 percent exposure latitude that fits within the envelope. Obviously, other rectangles can be drawn in the envelope depending on exposure process requirements. The process window for the 9.0 μm feature is contained within the process window for the 15 μm feature. This remains true for features up to 40 μm, the largest evaluated in this study. 500 mJ/cm<sup>2</sup> exposure gives the optimum performance for 9.0 μm features with a focus range in excess of 20 μm. Above 550 mJ/cm<sup>2</sup> exposure the focus latitude drops off quickly.

The top down SEM mask linearity results shown in Figure 3 are confirmed by the cross sectional SEM analysis. Excellent photoresist sidewalls were obtained over the entire range of spacewidths. No photoresist residue was observed at the bottom of any features. This problem observed in a previously published evaluation has been resolved through a change in the develop process [18]. A short duration highly aggressive photoresist GBL thinner cycle was added before the start of the development cycle to facilitate the removal of unexposed photoresist. Details of the develop process for SU8-10 appear in Table 3.

### 3.3 Futurrex NR9-8000

Futurrex NR9-8000 is a negative, polyhydroxy-styrene based photoresist designed for i-line applications. It uses an aqueous TMAH based developer. Previous evaluation of NR5-8000 on the Titan stepper showed minimal photo-sensitivity in the gh-line spectrum [18]. Since the Futurrex NR9-8000 photoresist is a negative acting photoresist, a film retention analysis was performed. The film retention analysis published in a previous study showed an average value of 95 percent of the pre-develop thickness measured over the exposure doses used for this study, indicating excellent film retention [18].

Wafers were imaged on the Saturn III stepper with exposure energies ranging from 1600 mJ/cm<sup>2</sup> to 2200 mJ/cm<sup>2</sup> and the focus offsets varied from -50 μm to +15 μm. Cross sectional SEM micrographs are shown in Figure 5a. Futurrex NR9-8000 demonstrated 29 μm resolution for isolated spaces with an aspect ratio of 3.3:1. The sidewall profiles varied considerably based on the feature size, and varied somewhat based on focus offset. The range of geometries in Figure 5b show the smallest feature, 20 μm, to be uncleared. The 29 μm feature is clear and shows some undercutting at both -20 and -35 focus offsets. The 34 μm lines show considerable undercut for -20 μm focus offset compared to much less pronounced undercut for a -35 μm focus offset. It is hypothesized that for this photoresist the develop process must be optimized for a single narrow range of CDs leaving larger geometries undercut and smaller geometries uncleared. This conflicts with the linearity results based on top down SEM data shown in Figure 3. The cross section SEM data suggests that there is no linear correlation between mask CDs and printed CDs for the NR9-8000 when profiles are considered. This photoresist was evaluated at 50 μm thickness

and was shown to be comparable to the SU-8 at that thickness [18]. At 100  $\mu\text{m}$  thickness the SU-8 resolves 14.3:1 aspect ratio features compared to 3.3:1 aspect ratios for the NR9-8000.

Figure 5b shows two Bossung plots based on top down SEM and generated through a focus and exposure matrix for NR9-8000 for 24  $\mu\text{m}$  and 29  $\mu\text{m}$  spacewidths. Process windows shown in Figure 5c based on these Bossung plots show a well behaved process window for the 24  $\mu\text{m}$  feature falling inside the process window for the 29  $\mu\text{m}$  feature. The results observed from cross sectional SEM analysis suggest a different conclusion. The top and bottom CDs are not well correlated and limited or no overlap exists between the process windows for various feature sizes. Here is an example of the failure of standard microelectronic CD metrology data to describe the more complex three dimensional structures observed in certain thick photoresists. The top down SEM results for CD measured through focus and exposure dose to generate Bossung plots yield an ambiguous and sometimes inaccurate view of cross sectional photoresist performance. As discussed earlier, wall angle measurements are not an effective way to differentiate photoresist performance for 100  $\mu\text{m}$  thick films. Better methods of quantifying profile variation and comparing very thick photoresists are suggested as areas for future work.

### 3.4 Clariant AZ PLP-100

Clariant AZ PLP-100 is a positive, novolac-based, broad spectral sensitivity photoresist. Wafers were imaged on the Titan II stepper with exposure energies ranging from 2600  $\text{mJ}/\text{cm}^2$  to 5000  $\text{mJ}/\text{cm}^2$  and the focus offsets varied from -50  $\mu\text{m}$  to +15  $\mu\text{m}$ . Cross sectional SEM micrographs of AZ PLP-100 are shown in Figure 6a. The smallest space that is cleared is 18  $\mu\text{m}$  (50 percent signal threshold) yielding a 5.4:1 aspect ratio. The SEM photos were all taken of exposures at a -5  $\mu\text{m}$  focus offset and 4200  $\text{mJ}/\text{cm}^2$  exposure dose. All cross section SEM photos exhibit a sloping foot at the base of the photoresist. The top of the photoresist shows a sharp flair and is probably the result of the aggressive development required to clear features in 100  $\mu\text{m}$  thick photoresist. Full photoresist height remains for the isolated space features shown. The curving foot is probably caused by a combination of aerial image position, softbake temperature, surface inhibition and multiple bakings.

Figure 6b shows Bossung plots for 38  $\mu\text{m}$  and 26  $\mu\text{m}$  features based on top down SEM data. Process windows shown in Figure 6c based on these Bossung plots show a well behaved process window for both feature sizes with the 26  $\mu\text{m}$  feature falling inside the process window for the 38  $\mu\text{m}$  feature. This remains true for the largest features evaluated for this study.

The mask linearity results from Figure 3 are validated by cross sectional SEM analysis with top and bottom geometries well correlated. However, because of the foot and slope reversal at the top of the features significantly different mask bias can result depending on the signal threshold chosen for CD SEM analysis. This result may lead to some confusion when attempting to decide upon a single bias to use for a photomask. The complex profiles observed in this photoresist do not lend themselves to the linear analysis generally used to describe photoresist profiles.

## 4.0 CONCLUSIONS

This paper has explored the performance of three ultra-thick photoresist for high aspect ratio MEMS and flipchip bump bond applications on the Ultratech Titan and Saturn family of steppers. Standard photoresist characterization techniques have been applied to MCC SU8-10, Futurrex NR9-8000 and Clariant AZ PLP-100. Cross sectional SEM analysis, Bossung plots and process window analysis were used to establish relative lithographic capabilities of each photoresist. The trade-off between the various photoresist chemistries were reviewed and compared with the process requirements for ultra-thick photoresist applications in MEMS and flipchip bump bonding.

A summary of recommended lithographic applications for the three photoresists is given in Table 6. It is clear that the SU8-10 offers the smallest feature resolution of the three photoresists with 14.3:1 aspect ratios possible in 100  $\mu\text{m}$  of photoresist. The SU8-10 has the further advantage of requiring the lowest exposure dose; an advantage for stepper throughput and overall cost of ownership. The profiles of the SU8-10 are nearly vertical and the linearity is the most consistent between the top down and cross section analysis of the three photoresists. The AZ PLP-100 resolved features as small as 18  $\mu\text{m}$ , however the sidewall profiles exhibited a curved foot as well as a sharp flair at the top. The optimum exposure dose for the AZ-PLP100 was 3000-3700  $\text{mJ}/\text{cm}^2$ ; much higher than the dose required for the SU8-10. The behavior of the Futurrex NR5-8000 degraded markedly for the 100  $\mu\text{m}$  thickness relative to the 50  $\mu\text{m}$  performance of the NR5-8000 explored in a previous study. At 50  $\mu\text{m}$  thickness aspect ratios as high as 5.5:1 were reported for this photoresist with profiles staying constant for a range of feature sizes. At 100  $\mu\text{m}$  thickness the NR5-8000 had a maximum aspect ratio of 3.3:1 and profiles varied considerably as a function of printed feature size. It is clear that better methods of describing and comparing the performance of thick photoresists are needed because of the complex nature of the photoresist profiles.

## 5.0 REFERENCES

1. J. Knutti, "Finding Markets For Microstructures", *Micromachining and Fabrication Process Technology IV Proceedings*, SPIE **3511**, 1998, p17-23.
2. R. Wechsung, N. Unal, "Market Analysis for Microsystems: an Interim Report From the Nexus Task Force", *Micro System Technologies 98 Proceedings*, December 3, 1998, pg. 275.
3. Nexus Report, "Market Analysis for Microsystems 1996-2002", October 1998.
4. M. Madou, "Fundamentals of Microfabrication", *CRC Press*, 1997, pg. 325-368.
5. J. Grasegger, "Rapid Prototyping of Microfluidic Structures with Nd:YAG-Laser Ablation", *Micro System Technologies 98 Proceedings*, December 3, 1998, pg. 439.
6. Lehr, "New Extensions of LIGA Technology," *Micromachine Devices*, November 1996.
7. M. Madou, *Fundamentals of Micromachining*, pg. 275-323.
8. E. Becker et al., "Production of Separation Nozzle Systems for Uranium Enrichment by a Combination of X-Ray Lithography and Galvanoplastics", *Naturwissenschaften*, **69** (1982), pg. 520-523.
9. L. Romankiw, I. Croll, M. Hatzakis, "Batch Fabricated Thin-Film Magnetic Recording Heads", *IEEE Trans. Magn.*, MAG-6 (1970), pg. 597-601.
10. P. Cheang, W. Staud, G. Newman, "A Low Cost Lithography Process for Flip Chip Applications in Advanced Packaging Industry," *Advanced Manufacturing Technologies Seminar*, 1997.
11. Lau, "Next Generation Low Cost Flip Chip Technologies," *46th Electronic Components & Technology Conference*, 1996.
12. S. J. Bart et. al., "Design Rules for a Reliable Surface Micromachined IC Sensor", 1995 *IEEE Internation Rel. Physics Proceedings*, 33rd Annual, April 1995, pg. 311-317.
13. N. Taniguchi, "Current Status in and Future Trends of Ultraprecision Machining and Ultrafine Materials Processing", *Annal. of the CIRP*, S573-582, 1983.
14. T. Higuchi and Y. Yamagata, "Micromachining by Machine Tools", *IEEE Microelectromechanical Systems Proceedings*, 1993.

15. Z. Mohammed, et. al., "1X Lithography for a Micromachined Accelerometer", *Micromachining and Microfabrication Process Technology III*, SPIE **3223**, 1997.
16. L. Thompson, C. G. Willson, M. Bowden, *Introduction to Microlithography*, Second Edition, American Chemical Society, 1994, pg. 71.
17. W. Flack, W. Fan, S. White, "The Optimization and Characterization of Ultra-thick Photoresist Films," *Advances in Resist Technology and Processing XV Proceedings*, SPIE **3333**, 1998.
18. W. Flack, W. Fan, S. White, "Characterization of Ultra-thick Photoresists for MEMS Applications Using a 1X Stepper", *Materials and Device Characterization in Micromachining Proceedings*, SPIE **3512**, 1998.
19. Flores, Flack, Dwyer, "Lithographic Performance of a New Generation i-line Optical System," *Optical/Laser Lithography VI Proceedings*, SPIE **1927**, 1993.

Parameter	Titan II	Saturn III
Reduction factor	1X	1X
Wavelength (nm)	390-450	355-375
Numerical aperture (NA)	0.32	0.365
Partial coherence ( $\sigma$ )	0.50	0.44
Wafer plane irradiance (mW/cm <sup>2</sup> )	1200	700

**Table 1:** Optical specifications of the lithography systems used in this study.

Photoresist	Mask bias ( $\mu\text{m}$ )	Data fit $R^2$
MCC SU8-10	-3.0	0.9991
Futurrex NR9-8000	-0.70	0.9987
AZ PLP-100	+8.4	0.9965

**Table 2:** Photoresist linearity based on the linearity regression analysis of Figure 3.

Process Step	Parameters	Equipment
Photoresist Coat	Dynamic dispense: 450 rpm for 5 seconds Spin: 700rpm for 15 seconds	Solitec 5110C Coater
Softbake	600 seconds at 70°C, hard-contact 25 minutes at 95°C, hard-contact	Solitec VBS-200
Post Exposure Bake	60 seconds at 50°C, then 600 seconds at 95°C	Solitec VBS-200
Develop	GBL thinner at 21°C 360 seconds immersion with agitation SU8-10 developer at 21°C 360 seconds immersion with agitation	Batch
Rinse	Rinse with SU8-10 developer for 30 seconds then gently air dry	Batch

**Table 3:** Process conditions for MCC SU8-10 photoresist.

Process Step	Parameters	Equipment
Photoresist Coat-1	Static dispense: 0 rpm for 10 seconds Spin: 500 rpm for 40 seconds	Solitec 5110C Coater
Softbake-1	120 seconds at 70°C, hard contact	Soletic VBS-200
Photoresist Coat-2	Static dispense: 0 rpm for 10 seconds Spin: 500 rpm for 40 seconds	Solitec 5110C Coater
Softbake-2	120 seconds at 70°C, hard contact 30 minutes at 110°C, hard contact	Soletic VBS-200
PEB	500 seconds at 100°C	Solitec VBS-200
Develop	RD6 developer at 21°C 360 seconds immersion with agitation, replace developer at 180 seconds	Batch
Rinse	DI water rinse for 60 seconds then gentle air dry	Batch

**Table 4:** Process conditions for Futurrex NR9-8000 photoresist.

Process Step	Parameters	Equipment
Adhesion Promotion	HMDS vapor prime	YES LP-3 Oven
Photoresist Coat-1	Static dispense: 0 rpm for 15 seconds Spin: 1100 rpm for 20 seconds	Solitec 5110C Coater
Softbake-1	60 seconds at 50°C, hard contact	Soletic VBS-200
Photoresist Coat-2	Static dispense: 0 rpm for 15 seconds Spin: 1100 rpm for 20 seconds	Solitec 5110C Coater
Softbake-2	300 seconds at 50°C, hard contact 600 seconds at 110°C, hard contact	Soletic VBS-200
Develop	AZ400K (1:3) at 25°C 18 minute immersion with agitation replace developer at 4 minute intervals	Batch
Rinse	DI water rinse for 30 seconds then gently air dry	Batch

**Table 5:** Process conditions for Clariant AZ PLP-100 photoresist.

Photoresists	AZ PLP-100	NR9-8000	MCC SU8-10
Stepper Model	Titan (gh-line)	Saturn (i-line)	Saturn (i-line)
Resolution ( $\mu\text{m}$ )	18	29	7.0
Nominal Dose ( $\text{mJ}/\text{cm}^2$ )	4200	1700	500
Exposure Latitude ( $\text{mJ}/\text{cm}^2$ )	3000-3700	1600-2000	475-560
Focus Latitude ( $\mu\text{m}$ )	-35 to +5	-32 to +10	-26 to -10
Reticle Bias ( $\mu\text{m}$ )	+8.4	-0.7	-3.0

**Table 6:** Recommended lithographic applications on Ultratech steppers in 100  $\mu\text{m}$  films for Clariant AZ PLP-100, Futurrex NR9-8000 and MCC SU8-10 photoresists.

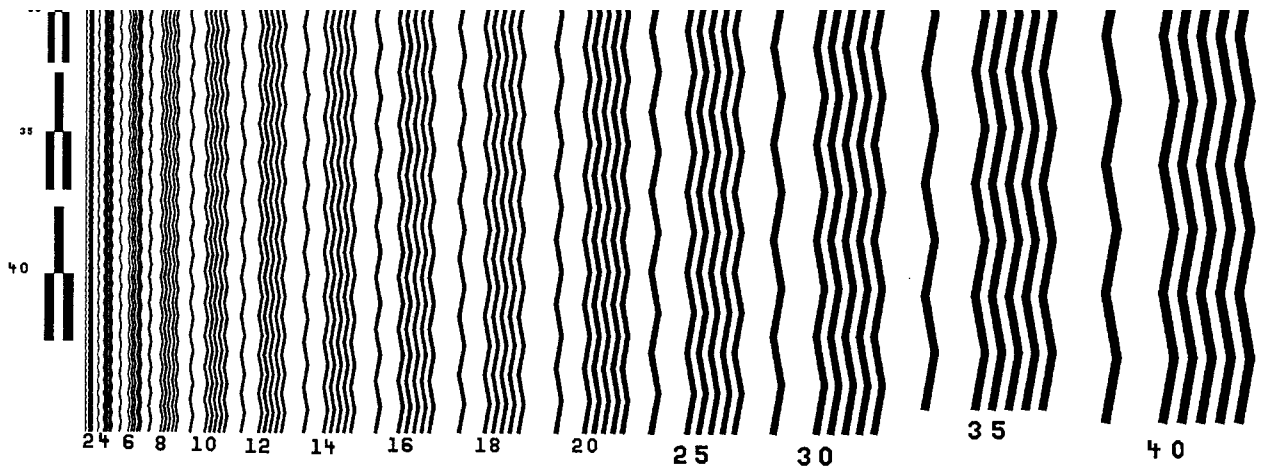


**Figure 1:** Partial view of the photomask layout showing vertical grouped and isolated lines from 2 to 40 μm in size. The long SEM lines are placed in a zigzag pattern to increase mechanical integrity of the photoresist.

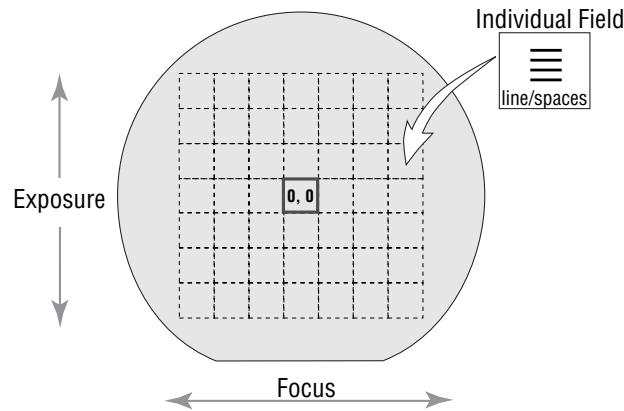


**Figure 2:** Wafer layout for the focus and exposure test matrix. A seven by seven field array was exposed with focus ranging in the horizontal axis and exposure dose ranging on the vertical axis.

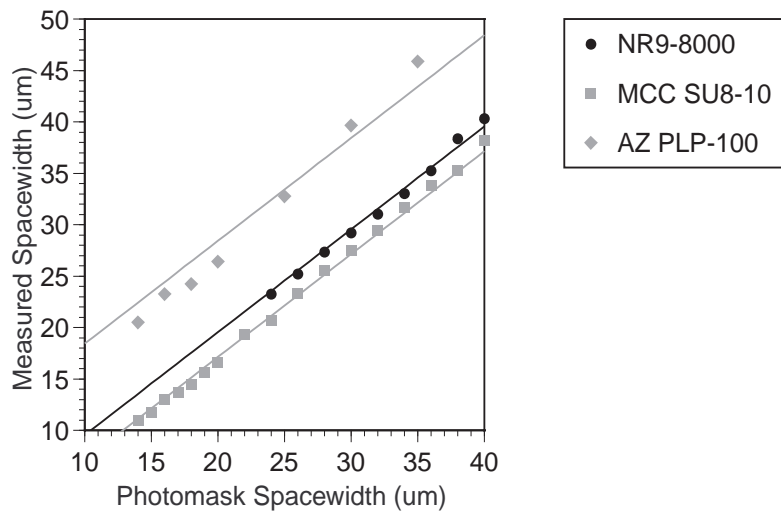
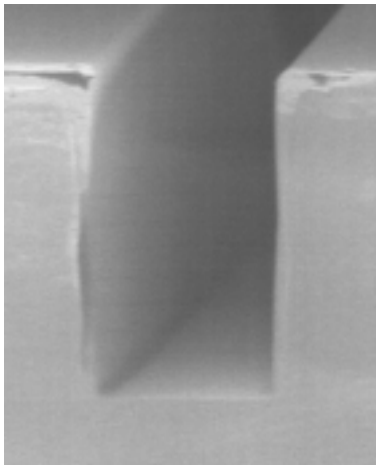
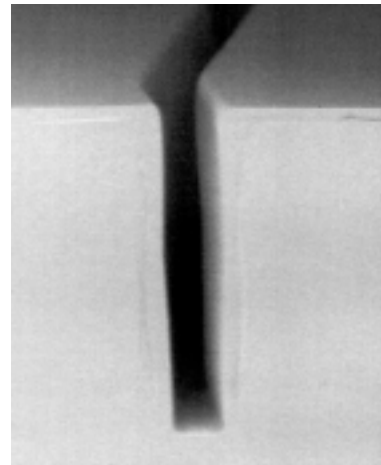


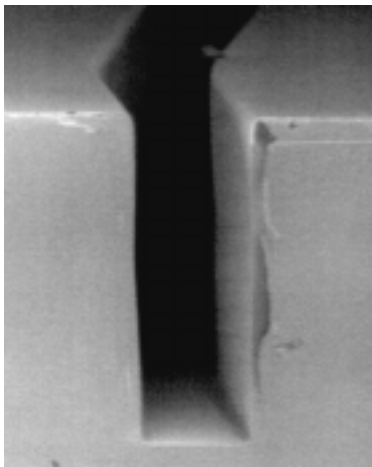
**Figure 3:** Mask linearity plot for AZ PLP-100, NR9-8000 and SU-8 photoresists. The reticle bias was determined for each photoresist by regression analysis and is summarized in Table 2.



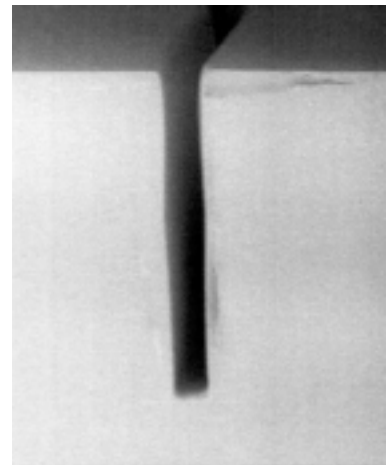
Spacewidth = 37  $\mu\text{m}$



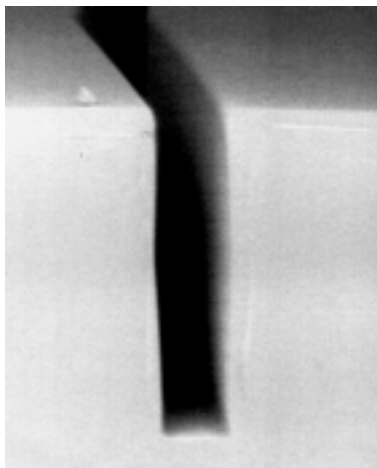
Spacewidth = 13  $\mu\text{m}$



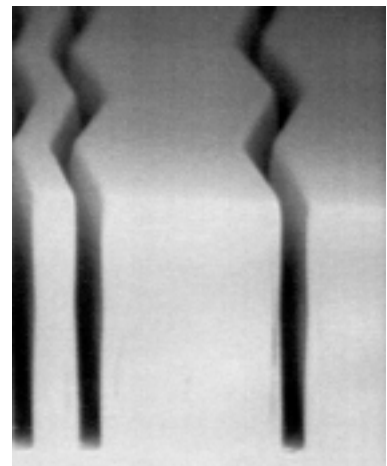
Spacewidth = 27  $\mu\text{m}$



Spacewidth = 9.0  $\mu\text{m}$



Spacewidth = 17  $\mu\text{m}$



Spacewidth = 7.0  $\mu\text{m}$

**Figure 4a:** Spacewidth linearity for 100  $\mu\text{m}$  thick MCC SU8-10 photoresist exposed at i-line. The exposure dose is 500  $\text{mJ}/\text{cm}^2$  and the focus offset is -20  $\mu\text{m}$ .

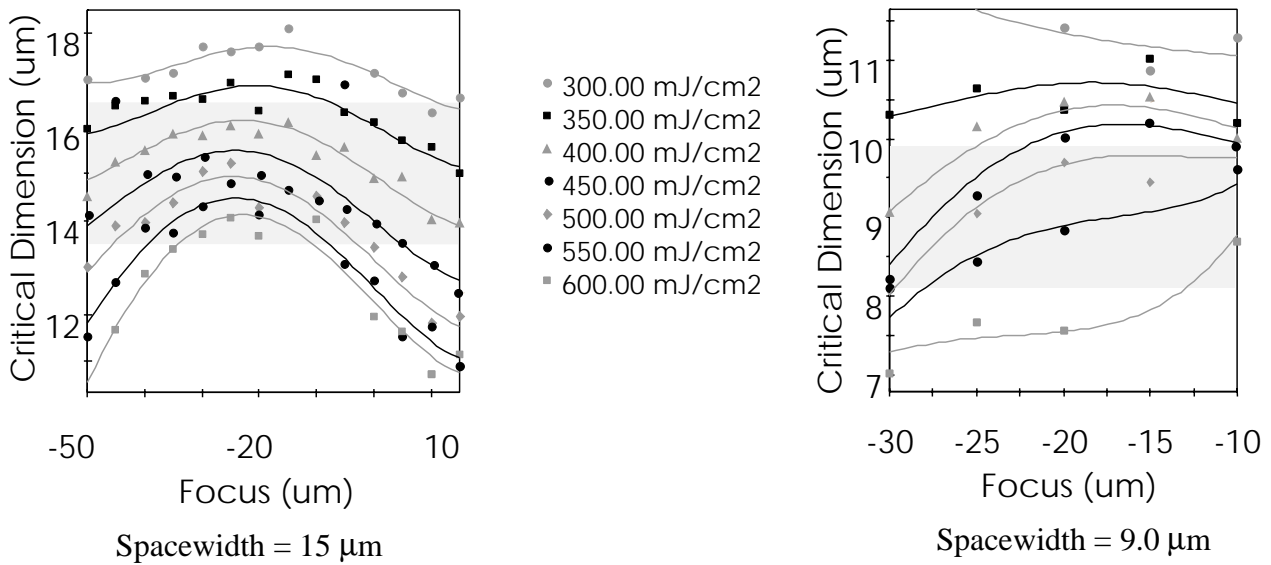


**Figure 4b:** Focus and exposure matrix for MCC SU8-10 photoresist exposed at i-line. The shaded rectangle shows  $\pm 10$  percent control limits based on the photoresist spacewidth size. The photomask size is biased by  $-3.0 \mu\text{m}$  based on the photomask linearity.

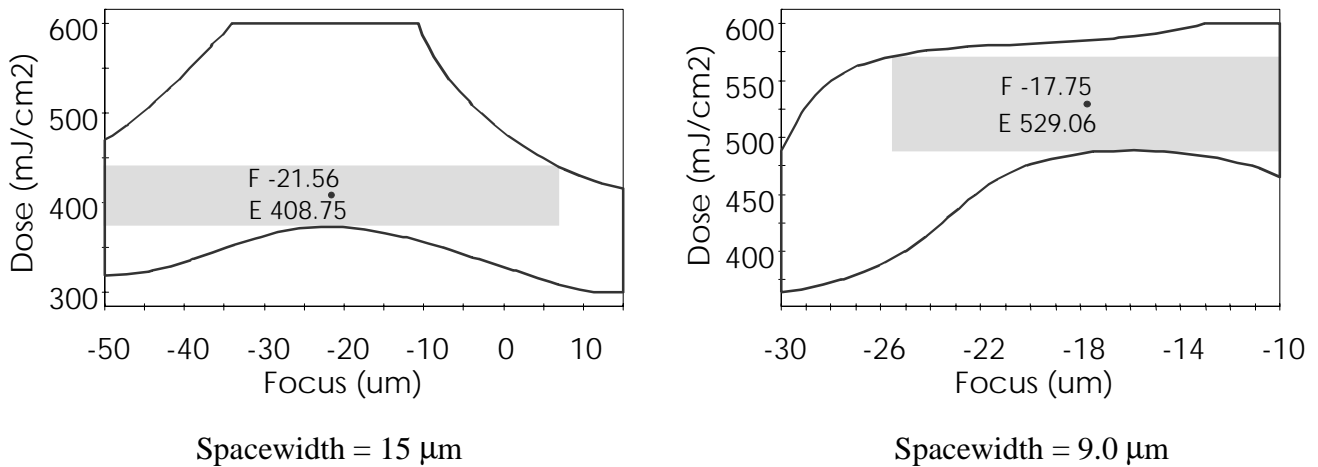
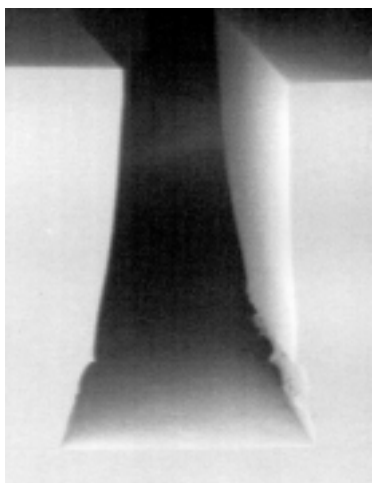
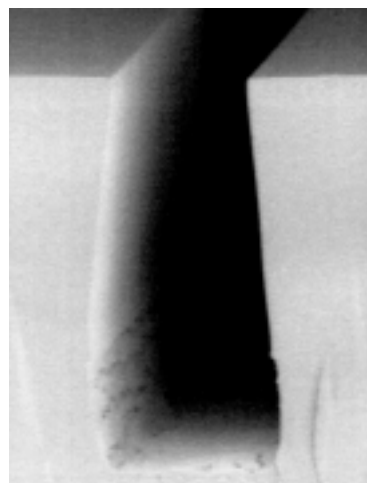


**Figure 4c:** Process window for MCC SU8-10 photoresist exposed at i-line. The process envelope shows  $\pm 10$  percent control limits based on the spacewidth size. The shaded rectangle shows the largest process window with a 15 percent exposure latitude. The photomask size is biased by  $-3.0 \mu\text{m}$  based on the photomask linearity. The nominal focus and exposure is for the center of the shaded rectangle.

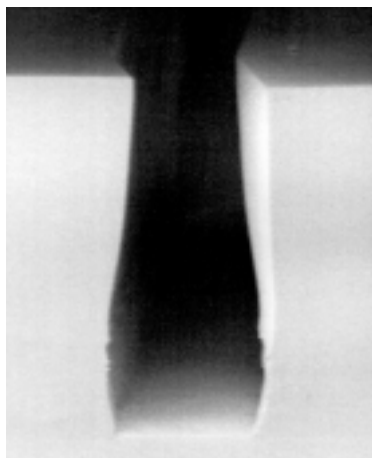


Focus = -20.0  $\mu\text{m}$

Spacewidth = 34  $\mu\text{m}$

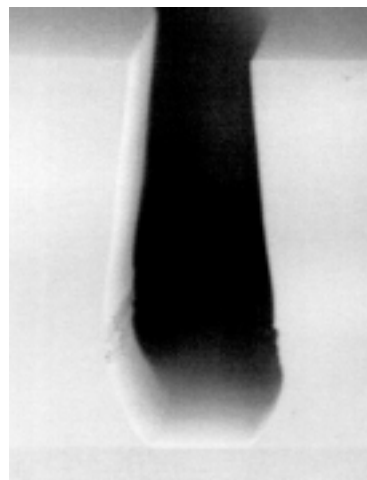


Focus = -35.0  $\mu\text{m}$

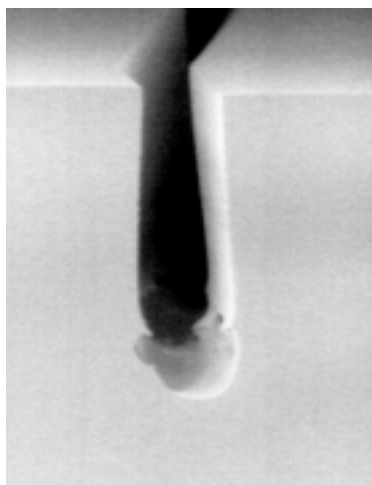


Focus = -20.0  $\mu\text{m}$

Spacewidth = 29  $\mu\text{m}$



Focus = -35.0  $\mu\text{m}$



Focus = -20  $\mu\text{m}$

Spacewidth = 19  $\mu\text{m}$

**Figure 5a:** Mask linearity for 100  $\mu\text{m}$  thick Futurrex NR9-8000 photoresist exposed at i-line. The exposure dose is 1700  $\text{mJ}/\text{cm}^2$  and the focus offsets are -20 and -35  $\mu\text{m}$ .

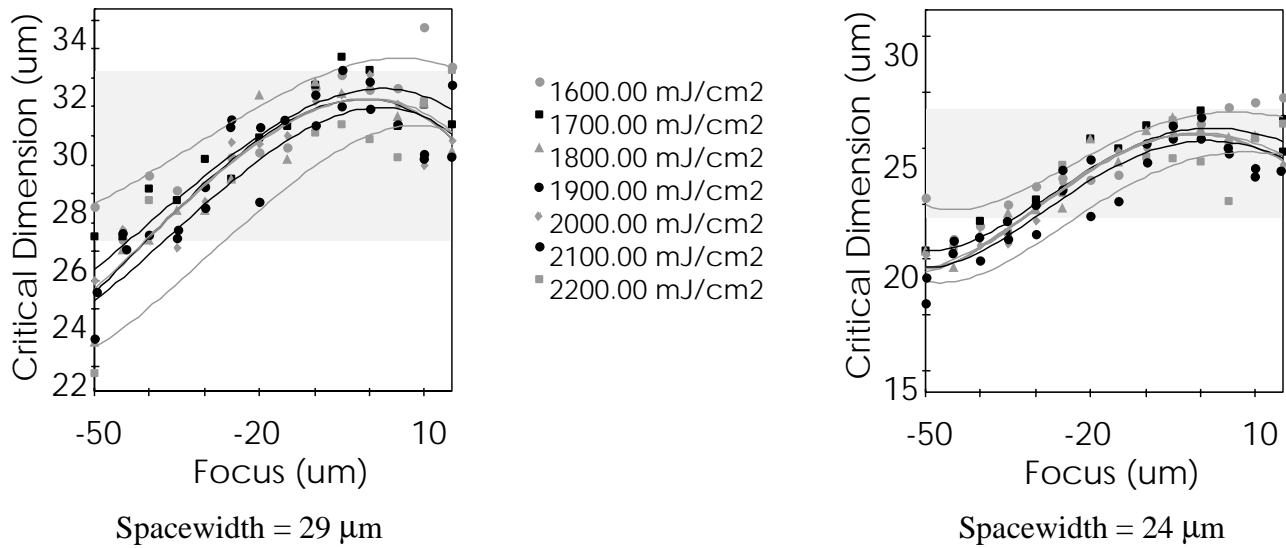


**Figure 5b:** Focus and exposure matrix for Futurrex NR9-8000 photoresist exposed at i-line. The shaded rectangle shows  $\pm 10$  percent control limits based on the photoresist spacewidth size. The photomask size is biased by  $-0.7 \mu\text{m}$  based on the photomask linearity.

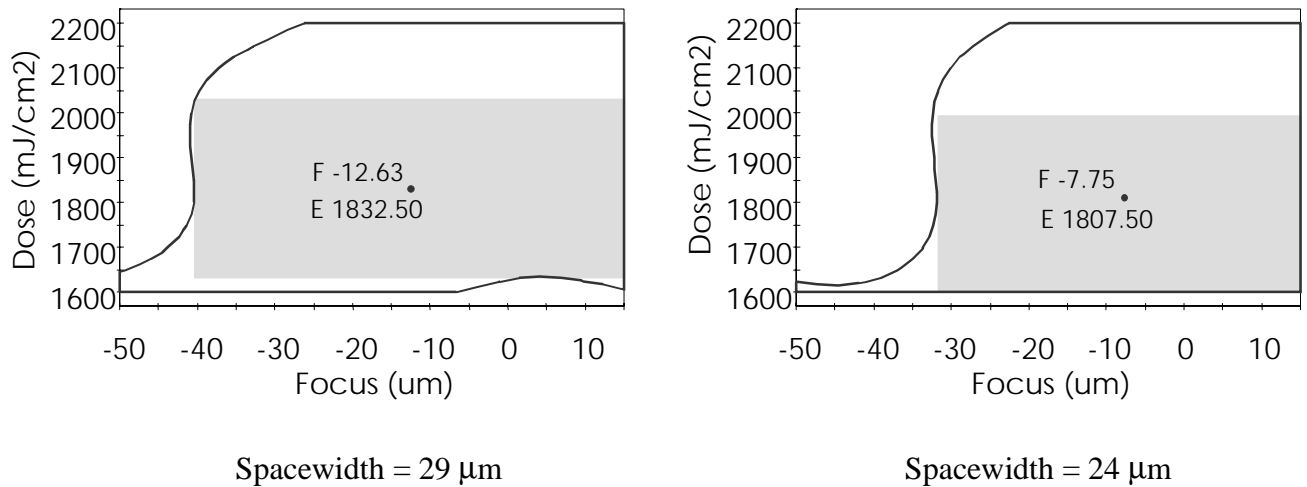
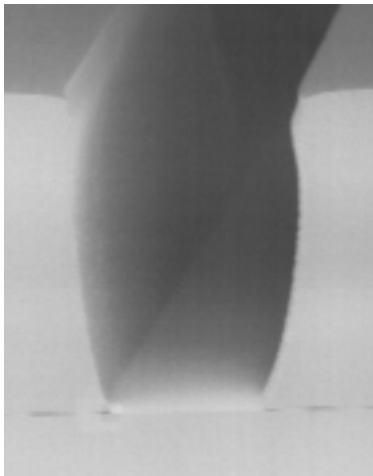
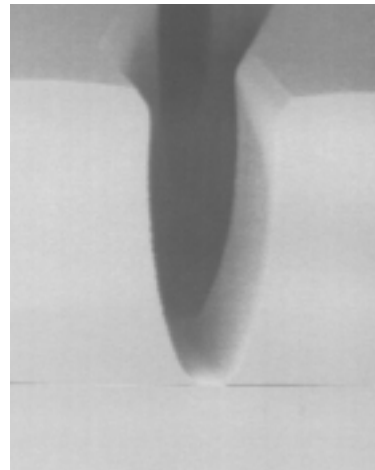


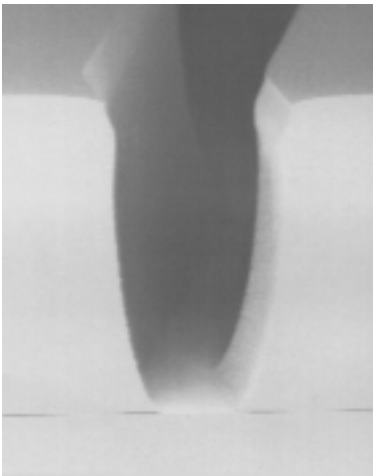
**Figure 5c:** Process window for Futurrex NR9-8000 photoresist exposed at i-line. The process envelope shows  $\pm 10$  percent control limits based on the spacewidth size. The shaded rectangle shows the largest process window with a 15 percent exposure latitude. The photomask size is biased by  $-0.7 \mu\text{m}$  based on the photomask linearity. The nominal focus and exposure is shown for the center of the shaded rectangle.



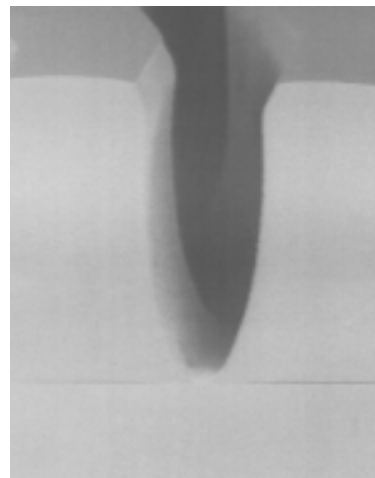
Spacewidth = 48  $\mu\text{m}$



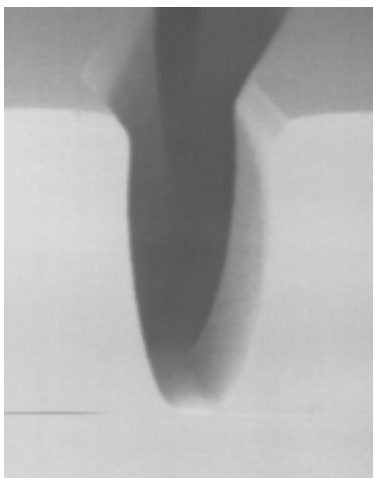
Spacewidth = 22  $\mu\text{m}$



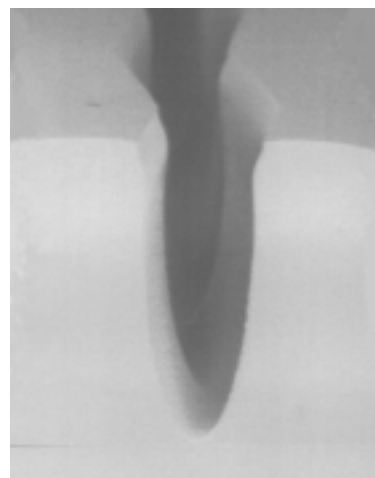
Spacewidth = 33  $\mu\text{m}$



Spacewidth = 20  $\mu\text{m}$



Spacewidth = 26  $\mu\text{m}$



Spacewidth = 18  $\mu\text{m}$

**Figure 6a:** Mask linearity for 100  $\mu\text{m}$  thick Clariant AZ PLP-100 photoresist exposed at gh-line. The exposure dose is 4200  $\text{mJ}/\text{cm}^2$  and the focus offset is -5  $\mu\text{m}$ .

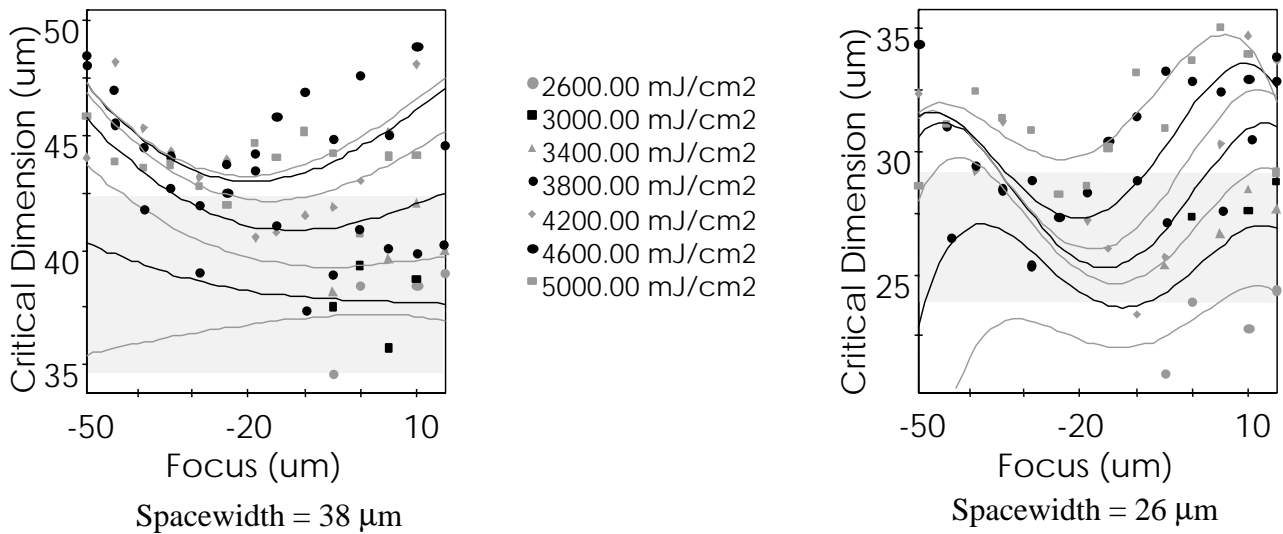


**Figure 6b:** Focus and exposure matrix for Clariant AZ PLP-100 photoresist exposed at gh-line. The shaded rectangle shows  $\pm 10$  percent control limits based on the photoresist spacewidth size. The nominal photoresist size is biased by  $+8.4 \mu\text{m}$  based on the photomask linearity.

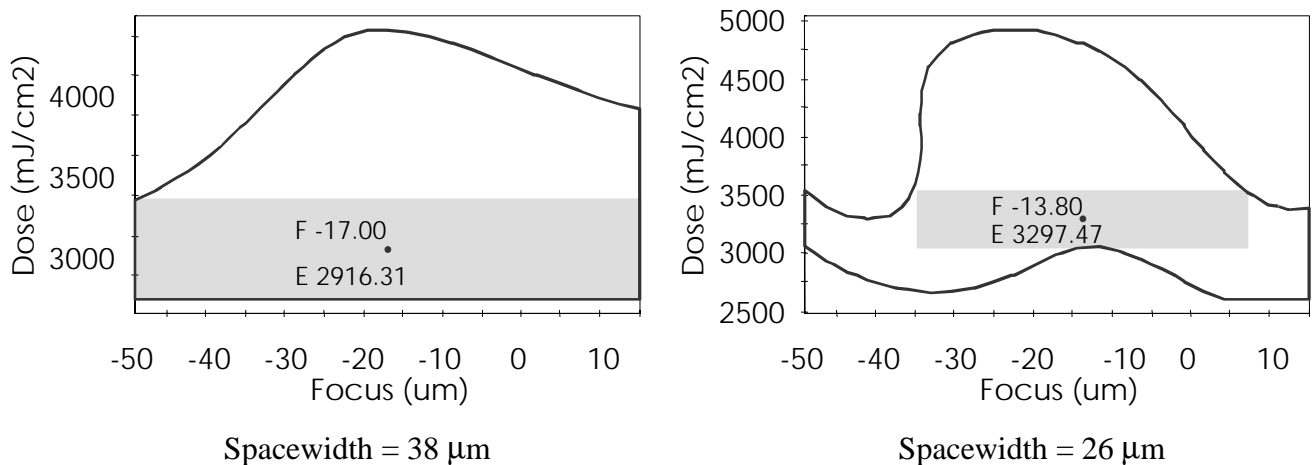


**Figure 6c:** Process window for Clariant AZ PLP-100 photoresist exposed at gh-line. The process envelope shows  $\pm 10$  percent control limits based on the spacewidth size. The shaded rectangle shows the largest process window with a 15 percent exposure latitude. The photomask size is biased by  $+8.4 \mu\text{m}$  based on the photomask linearity. The nominal focus and exposure is shown for the center of the shaded rectangle.